
UNDERSTANDING THE DESIGN PRINCIPLES OF LINK PREDICTION IN DIRECTED SETTINGS *

Jun Zhai, Muberra Ozmen, Thomas Markovich
Block, Inc.
{junzhai, muberra, tmarkovich}@block.xyz

ABSTRACT

Link prediction is a widely studied task in *Graph Representation Learning (GRL)* for modeling relational data. The early theories in GRL were based on the assumption of a symmetric adjacency matrix, reflecting an undirected setting. As a result, much of the following state-of-the-art research has continued to operate under this symmetry assumption, even though real-world data often involve crucial information conveyed through the direction of relationships. This oversight limits the ability of these models to fully capture the complexity of directed interactions. In this paper, we focus on the challenge of directed link prediction by evaluating key heuristics that have been successful in undirected settings. We propose simple but effective adaptations of these heuristics to the directed link prediction task and demonstrate that these modifications produce competitive performance compared to the leading *Graph Neural Networks (GNNs)* originally designed for undirected graphs. Through an extensive set of experiments, we derive insights that inform the development of a novel framework for directed link prediction, which not only surpasses baseline methods but also outperforms state-of-the-art GNNs on multiple benchmarks.

1 Introduction

Link prediction is a task that seeks to uncover missing connections (*e.g.* links), between entities (*e.g.* vertices) in a graph, and has many industrial applications. For example, an e-commerce platform might represent their users and items as vertices, and the transactions users make as edges from user to item. In this setting, a recommendation system that predicts items that users might like to buy can readily be cast as a link prediction task [Chamberlain et al., 2022, Wang et al., 2023]. Beyond direct applications, link prediction is often used in unsupervised settings to construct vertex representations that can then be used in various downstream tasks, such as fraud or toxicity detection [Pal et al., 2020, El-Kishky et al., 2022, Liu et al., 2020, Zhang et al., 2022].

Various methodologies for link prediction have been developed and can be broadly classified into three categories. The first category, *similarity-based heuristics*, involves computing a score for each pair of nodes to quantify their similarity [Wang et al., 2007]. These scores are then ranked, with higher scores indicating a greater likelihood of connection between node pairs. The second category encompasses *probabilistic and maximum likelihood models* [Wang et al., 2007, Clauset et al., 2008, Guimerà and Sales-Pardo, 2009]. Although these models have demonstrated effectiveness on smaller datasets, they tend to be computationally intensive and face scalability challenges in large real-world graphs. The third category includes *node representation learning methods*, where an *encoder* learns to represent each node as a vector in an embedding space, and a *decoder* processes pairs of node embeddings to generate a score that quantifies the likelihood of a link existing. These embeddings are optimized so that nodes with similar neighborhood structures are represented similarly in the embedding space. Node representation methods can be further divided into three subcategories based on the choice of encoder: *random walk-based approaches* [Perozzi et al., 2014, Trouillon et al., 2016, Cao et al., 2018, Kazemi and Poole, 2018], *matrix decomposition techniques* [Acar et al., 2009,

**Citation:* Jun Zhai, Muberra Ozmen, and Thomas Markovich. 2025. Understanding the Design Principles of Link Prediction in Directed Settings. In Companion Proceedings of the ACM Web Conference 2025 (WWW Companion '25), April 28-May 2, 2025, Sydney, NSW, Australia. ACM, New York, NY, USA, 12 pages. <https://doi.org/10.1145/3701716.3717803>.

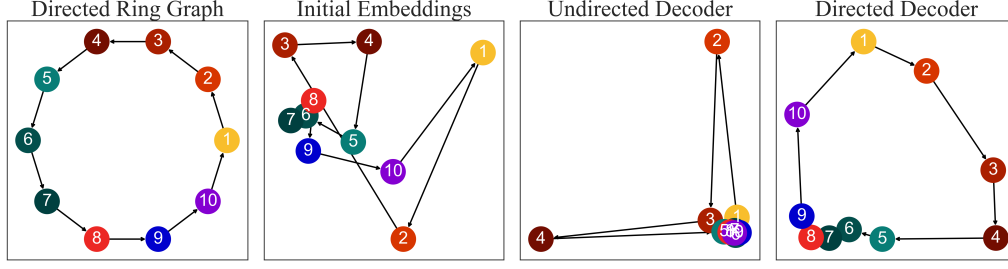


Figure 1: **An illustrative evaluation demonstrating the impact of incorporating directionality into the design of predictive models.** We generate a directed ring graph $\mathcal{G} = (\mathcal{V}, \mathcal{E})$. Each node $u \in \mathcal{V}$ is initialized with a two-dimensional embedding $\mathbf{e}_u^{(0)}$. We then train GraphSage [Hamilton et al., 2017], to update these embeddings using two different decoders: (1) a undirected decoder, and (2) a directed decoder, to perform link prediction. By visualizing the output node embeddings in both cases, we observe that the structural representation of nodes is significantly enhanced when using a directed decoder, emphasizing the importance of directionality in the model design.

Kazemi and Poole, 2018], and *Graph Neural Networks (GNNs)* [Kipf and Welling, 2016, Hamilton et al., 2017, Ying et al., 2018, Veličković et al., 2017].

Although link prediction is valuable across many applications, most widely used methods assume that links are undirected. In many settings, this assumption makes sense. For example, an edge in the Facebook friendship graph will be undirected, because friendships are bidirectional on the platform. As a result, it is common to transform directed graphs into undirected ones. However, this undirected transformation does not make sense in all settings because an edge’s directionality can denote the semantics of that edge, which is often crucial for accurately modeling interactions.

Intuitively, directed edges allow us to differentiate a node’s role as either a source or a target within a network, which provides finer granularity when modeling interactions. In many real-world contexts, this asymmetry is meaningful. For instance, consider a transaction network where the goal is to identify fraudulent behavior. Suppose there are three types of participants: a parent, a teenager, and a fraudster. Let’s assume the model aims to understand the identity and behavior of the teenager. A money transfer from a parent to a teenager represents one type of pattern, while a transfer from a teenager to a fraudster at the same monetary amount represents another. If we look at a scenario where the teenager is receiving money from the parent, this pattern might be considered safe—such as receiving an allowance. However, if the teenager is instead sending the same amount to a fraudster, this could be a red flag. By taking into account the direction of these transactions, we can more effectively distinguish between benign and suspicious patterns. In a directed setting, the directionality conveys vital information about who initiates and who receives a transaction, which can significantly impact downstream predictions. Conversely, if we convert the originally directed network into an undirected one by symmetrizing the adjacency matrix, the sender/receiver roles of the teenager in these transactions would be lost, potentially leading to a misinterpretation of the interactions and harming predictive performance.

To make this point clear, we have constructed a directed ring graph and present it in Figure 1, as well as embeddings generated using both an undirected and a directed graph decoder. We clearly observe that the asymmetric, or directed, decoder is more capable of replicating the expected planar positioning, while the undirected decoder generates a set of embeddings where almost all vertices collapse together in the embedding space. This example helps us to develop the intuition that using undirected link predictors in directed settings may lead to poor performance.

In this paper, we take this intuition and make it concrete by exploring the problem of directed link prediction. Along the way, we gain insights into the design principles needed for the development of link predictors that are applicable to directed settings. The key contributions of our work are as follows:

- We establish a **robust comparison framework** by constructing three types of baseline models: heuristic approaches, Multi-Layer Perceptron (MLP), and GNN based models and their variants for directed settings.
- We conduct extensive ablation experiments to extend the known **design principles** of link prediction to include their directed variants, and study the impact of directionality on the predictive performance for each such design principle.
- Based on the design principles determined, we develop DirLP, a **novel model for directed link prediction** that significantly outperforms the baseline models.

This work not only establishes a new state-of-the-art in directed link prediction but also offers actionable insights that inform the design of future models. Our contributions aim to bridge the gap between undirected and directed link prediction research, providing strong foundations for future work in this important area.

2 Related Work

For the review of literature, we focus on *similarity-based heuristics* for link prediction, due to their practical applicability, and *Graph Neural Networks (GNNs)*, which represent the state-of-the-art in the field.

Similarity-based Heuristics. A variety of similarity-based heuristics have been developed for the task of link prediction, primarily focusing on quantifying node similarity to predict the likelihood of a connection. One of the earliest and simplest methods is the *Common Neighbors (CN)* heuristic, where the number of shared neighbors between two nodes is used as an indicator of their likelihood to form a link. Extensions of this idea include the *Jaccard Index (JI)* and *Adamic-Adar index (AA)*, which provide weighted variations by considering the degree of shared neighbors Adamic and Adar [2003], Liben-Nowell and Kleinberg [2007]. The *Preferential Attachment (PA)* heuristic, based on the idea that high-degree nodes are more likely to attract additional links, is another widely used method Newman [2001]. *Local Path index (LP)* [Lü et al., 2009] expands upon the idea of common neighbors by considering paths of length two between node pairs. It balances between global and local information, providing a broader view of node similarity while still being computationally feasible for large graphs. *Resource Allocation index (RA)* [Zhou et al., 2009] is another similarity-based measure, where the likelihood of a link is determined by how resources (or connections) are shared between two nodes via their common neighbors. It gives higher weight to common neighbors with lower degrees, assuming that connections from lower-degree nodes are more significant. While these heuristics are computationally efficient and effective in many settings, they are primarily designed for undirected graphs and tend to struggle when applied to directed graphs. These methods also assume that local structural properties of the graph are sufficient for prediction, limiting their ability to capture more complex relational patterns. Despite these limitations, similarity-based heuristics remain popular due to their simplicity and interpretability, often serving as strong baselines for more advanced models like GNNs.

Graph Neural Networks (GNNs). Most of the popular GNNs [Kipf and Welling, 2016, Hamilton et al., 2017, Veličković et al., 2017, Ying et al., 2018] primarily focus on node representation in undirected graphs. Several studies have specifically addressed various aspects of directed graphs. For example, GatedGCN [Li et al., 2015], which employs separate aggregations for in-neighbors and out-neighbors in directed graphs, has proven effective for solving the genome assembly problem [Vrček et al., 2022]. Additionally, research has aimed to generalize spectral convolutions for directed graphs Ma et al. [2019], Monti et al. [2018], Tong et al. [2020b,a]. A notable contribution is made by Zhang et al. [2021b], who present a spectral method that utilizes a complex matrix for graph diffusion, where the real part represents the undirected adjacency and the imaginary part captures the edge direction. Building on their work, Geisler et al. [2023] proposed a positional encoder that integrates transformers into directed graphs. More recently, Rossi et al. [2024] emphasized that effective link prediction in directed graphs necessitates distinct aggregation strategies for incoming and outgoing edges to fully leverage directional information. They proposed a novel and generic *Directed Graph Neural Network (Dir-GNN)* that can be integrated with any message-passing neural network by implementing separate aggregations of incoming and outgoing edges.

Once the learned node embeddings are obtained, the link prediction problem can be framed as a supervised binary classification task. In this context, the input consists of a pair of node embeddings corresponding to the link of interest, while the output is a score that quantifies the probability of the existence of that link. Various decoders have been proposed to achieve this classification, each with distinct methodologies. One of the simplest and most widely used decoders is the dot product decoder [Kipf and Welling, 2016]. However, this method fails to account for the directionality of links since the dot product is commutative. For instance, in a transactional context, the likelihood of person A transferring money to person B is treated the same as that of person B transferring money to person A, which hinders accurate predictions of money flow. To address the limitations of the dot product, Bilinear Decoders introduce a learned weight matrix, providing a more nuanced approach to edge prediction [Yang et al., 2014]. Another method for quantifying the similarity between two nodes is the distance-based decoder, which predicts edge existence based on the distance between node embeddings [Ou et al., 2016]. Matrix factorization-based decoders decompose the adjacency matrix into low-rank matrices representing node embeddings. The reconstructed adjacency matrix can then be used for link prediction [Tang et al., 2015]. Neural Tensor Network (NTN) [Socher et al., 2013] replaces the standard linear layer with a bilinear tensor layer, directly relating the two nodes. A novel decoder inspired by Newton’s theory of universal gravitation was introduced by Salha et al. [2019]. This approach uses node embeddings to reconstruct asymmetric relationships, facilitating effective directed link prediction.

3 Background and Preliminaries

In this section we introduce the notation employed throughout the paper in addition to metrics and datasets used for experiments. Next, we provide an overview of two main frameworks adapted to address directed link prediction problem in our analysis: (1) similarity-based heuristics and (2) Graph Neural Networks (GNNs).

Notation. Given a graph $\mathcal{G} = (\mathcal{V}, \mathcal{E})$ where \mathcal{V} and \mathcal{E} denote the set of vertices and edges respectively, *directed link prediction* refers to the task of predicting the existence of an edge *from* $u \in \mathcal{V}$ *to* $v \in \mathcal{V}$. The adjacency matrix of \mathcal{G} is denoted by \mathbf{A} , where $\mathbf{A}_{uv} = 1$ if there is a directed edge from node u to v , and $\mathbf{A}_{uv} = 0$, otherwise. Additionally, we denote the neighbourhood of a given node u as $\mathcal{N}(u)$ throughout the paper. Each node $u \in \mathcal{V}$ is associated with a feature vector $\mathbf{x} \in \mathbb{R}^d$ where d is the feature dimensionality.

Metrics. In general, to evaluate the prediction performance of a given method, the set of edges is divided into disjoint sets of training and testing splits; $\mathcal{E}_{\text{train}}$ and $\mathcal{E}_{\text{test}}$, respectively. In this paper, we evaluate the predictive performance mainly by mean reciprocal rank (MRR), which is calculated as the average of the reciprocal ranks of the true positives in the test set. The MRR is formulated as follows:

$$\text{MRR} = \frac{1}{|\mathcal{E}_{\text{test}}|} \sum_{(u,v) \in \mathcal{E}_{\text{test}}} \frac{1}{\text{rank}(u, v)}, \quad (1)$$

where $\text{rank}(u, v)$ is the rank of the true link (u, v) among possible candidate links involving node u .

Datasets. In our experiments, we evaluate directed link prediction performance of various approaches using six benchmark datasets: CORA [Yang et al., 2016], CITESEER [Yang et al., 2016], CHAMELEON [Rozemberczki et al., 2021], SQUIRREL [Rozemberczki et al., 2021], BLOG [He et al., 2022], WIKICS [Mernyei and Cangea, 2020]. All datasets are directed and come from the PYTORCH GEOMETRIC SIGNED DIRECTED software package [He et al., 2024]. We use the directed version of CORA and CITESEER and not their commonly used undirected versions. The details regarding datasets are provided in Appendix A.

3.1 Similarity-based Heuristics

In general, similarity-based heuristic methods used for link prediction assign a similarity score $S(u, v)$ for each pair of nodes, such that $S(u, v)$ serves as an estimator on the likelihood of a link between node u and node v . For example, the Resource Allocation (RA) heuristic score between node u and v is calculated as follows:

$$S_{\text{RA}}(u, v) = \sum_{t \in \mathcal{N}(u) \cap \mathcal{N}(v)} \frac{1}{|\mathcal{N}(t)|}. \quad (2)$$

By definition, RA is a symmetric score function, i.e. $S_{\text{RA}}(u, v) = S_{\text{RA}}(v, u)$. In order to adapt the existing similarity scores into directed settings, we utilize *directed neighborhood operator*. Let $\mathcal{N}_{\text{in}}(u)$ ($\mathcal{N}_{\text{out}}(u)$) consists of all nodes that have a directed edge pointing toward (originating from) node u . Formally:

$$\mathcal{N}_{\text{in}}(u) = \{v \in \mathcal{V} \mid (v, u) \in \mathcal{E}\}, \quad \mathcal{N}_{\text{out}}(u) = \{v \in \mathcal{V} \mid (u, v) \in \mathcal{E}\}. \quad (3)$$

Using $\mathcal{N}_{\text{in}}(\cdot)$ and $\mathcal{N}_{\text{out}}(\cdot)$, one can define four variants of common neighbourhood for a given node pair u and v by $\mathcal{N}_{d_u}(u) \cap \mathcal{N}_{d_v}(v)$ where $d_u, d_v \in \{\text{in}, \text{out}\}$. For example, given the set of nodes that has an incoming link from u and has an outgoing link to v , the corresponding RA would be calculated as follows:

$$S_{\text{RA}, \text{in-out}}(u, v) = \sum_{t \in \mathcal{N}_{\text{in}}(u) \cap \mathcal{N}_{\text{out}}(v)} \frac{1}{|\mathcal{N}(t)|}. \quad (4)$$

More details regarding the individual methods used in our experiments are provided in Appendix B.

3.2 Graph Neural Networks (GNNs)

Encoders. Most common form of encoder used in GNNs is *Message Passing Neural Networks (MPNNs)* in which vector-based messages are passed between nodes and then updated through neural networks to generate node embeddings. MPNNs initialize a set of the hidden node embeddings $\mathbf{h}_u^{(0)}, \forall u \in \mathcal{V}$ by input features, i.e., $\mathbf{h}_u^{(0)} = \mathbf{x}_u$. At the k^{th} iteration of message passing hidden embeddings $\mathbf{h}_u^{(k)}$ for each node $u \in \mathcal{V}$ are updated as follows:

$$\mathbf{h}_u^{(k+1)} = f_{\text{update}}\left(\mathbf{h}_u^{(k)}, f_{\text{aggregate}}\left(\left\{\mathbf{h}_v^{(k)}, \forall v \in \mathcal{N}(u)\right\}\right)\right), \quad (5)$$

where $f_{\text{update}}(\cdot)$ and $f_{\text{aggregate}}(\cdot)$ are choice of differentiable functions. The final hidden embeddings are used as the output node embeddings $\mathbf{e}_u^{(0)}, \forall u \in \mathcal{V}$:

$$\mathbf{e}_u = \mathbf{h}_u^{(K)}, \forall u \in \mathcal{V}, \quad (6)$$

where K denotes the total number of update layers. In the functional form, an MPNN can be summarized as follows:

$$f_{\text{MPNN}} : \mathcal{G} = (\mathcal{V}, \mathcal{E}) \text{ and } \mathbf{x}_u, \forall u \in \mathcal{V} \mapsto \mathbf{e}_u, \forall u \in \mathcal{V}. \quad (7)$$

In terms of link prediction task, MPNNs serve as an encoder that maps structural information of the graph together with node features into a set of node embeddings.

Decoders. In the context of link prediction the decoder maps the embeddings for a given link to an individual score that corresponds to its likelihood to exist. For edge-wise link-prediction it is common to use one of two link predictors: the dot product (DP) $f_{\text{DP}}(v_i, v_j) = \sigma(\mathbf{e}_i^T \mathbf{e}_j)$ and the hadamard product (HMLP) $f_{\text{HMLP}}(v_i, v_j) = f_{\text{MLP}}(\mathbf{e}_i \odot \mathbf{e}_j)$. Both of these decoders are symmetric, (i.e. $f(v_i, v_j) = f(v_j, v_i)$), which is a desirable property in undirected graphs but might not be so desirable in undirected settings. It is straight forward to extend both DP and HMLP to directed settings through the insertion of a learnable matrix that looks spiritually like a learnable metric tensor. Doing so, we introduce two variants we term matrix dot product (mDP), $f_{\text{mDP}}(v_i, v_j) = \sigma(\mathbf{e}_i^T \mathbf{W} \mathbf{e}_j)$, and matrix HMLP, $f_{\text{mHMLP}}(v_i, v_j) = f_{\text{MLP}}(\mathbf{W} \mathbf{e}_i \odot \mathbf{e}_j)$, where \mathbf{W} is a learnable matrix. In addition, we define a trivially asymmetric decoder named Concat MLP (CMLP) and its matrix extension, matrix Concat MLP (mCMLP), defined as:

$$f_{\text{CMLP}} = f_{\text{MLP}}(\mathbf{e}_i \parallel \mathbf{e}_j) \text{ and } f_{\text{mCMLP}} = f_{\text{MLP}}(\mathbf{W} \mathbf{e}_i \parallel \mathbf{e}_j). \quad (8)$$

4 Analysis of Directionality for Link Prediction

In this section, we consider each of the design principles independently and perform experiments that allow us to understand the impact of directionality on each one. All experiments are performed on three different datasets: CORA, CHAMELEON, and BLOG. The results are averaged over ten runs, and the relevant hyperparameters are optimized using OPTUNA [Akiba et al., 2019].²

Directed vs Undirected Graph Encoders. Traditionally, the form and structure of the graph encoder have been the main area of focus in the GNN literature. Thus, we explore multiple GNN encoding architectures to understand the extent to which directionally aware graph encoders impact the predictive performance. We constructed an experiment where comparing two standard graph encoders - a GCN and GraphSAGE - with a directionally aware convolution, DirGNN. We performed this comparison by holding the decoder fixed and conducting a hyperparameter search over the relevant hyperparameters of the encoder itself. We present the results of the experiment in Table 1.

We observe that in two of three datasets, DirGNN performs better than the other encoders. It is interesting to note that the "uplift offered by more complex encoders provides only modest gains. This suggests that in directed settings, DirGNN is a sensible first choice as a graph encoder because it either performs better than others, or is within the error bars of the best.

Table 1: Encoder comparisons in terms of MRR.

Encoder	CORA	CHAMELEON	BLOG
GCN	0.401±0.062	0.595±0.058	0.283±0.039
GraphSage	0.414±0.077	0.603±0.062	0.275±0.027
DirGNN	0.503±0.088	0.609±0.026	0.278±0.024

Directed vs Undirected Graph Decoders. Because link prediction is traditionally viewed as an edge-wise prediction task with a link predictor taking the form $f(v_i, v_j) \rightarrow \mathbb{R}^+$, we next explore whether learning a link predictor with an asymmetric decoder (e.g., $f(v_i, v_j) \neq f(v_j, v_i)$) leads to better predictive performance.

To explore this, we constructed an experiment where the encoder was held fixed, and varied the decoder over two symmetric and four asymmetric decoders. For mathematical definitions of all decoders, please see Section 3.2. The results of this experiment are reported in Table 2. We observe that asymmetric decoders outperform symmetric ones across all three datasets, confirming our intuition that asymmetry is an important property to capture. Within the asymmetric decoders, we find that both mHMLP and CMLP outperform the others. Because mHMLP amounts to learning a pseudo-metric which can be unstable due to the many possible degeneracies, we use CMLP in the subsequent work.

Directed vs Undirected Labeling Tricks. Labeling tricks are one technique for breaking the node-automorphism symmetry which limits the expressivity of GNNs for link prediction Zhang et al. [2021a]. To do this, the node-features of a vertex are augmented by labels that connote some structural information. Popular labeling tricks include distance encoding [Li et al., 2020] and double radius node labeling [Zhang and Chen, 2018]. However, in this work, we consider only the directed extension of distance encoding due to its simplicity. Indeed, the directed extension of the distance encoding described in [Li et al., 2020] simply involves computing the distance between two vertices in a directed

²In the ablation study results presented in Tables 1-5, the best-performing version for each dataset is highlighted in orange.

Table 2: Decoder comparisons in terms of MRR.

<i>Decoder</i>	CORA	CHAMELEON	BLOG
DP	X±X	0.303±0.021	0.115±0.016
HMLP	0.178±0.046	0.261±0.047	0.113±0.024
CMLP	0.500±0.087	0.289±0.102	0.160±0.023
mDP	0.247±0.066	0.214±0.095	0.105±0.028
mHMLP	0.621±0.489	0.320±0.066	0.147±0.055
mCMLP	0.248±0.072	0.136±0.082	0.131±0.023

fashion as defined in Equation 9. It is canonical to define a maximum distance to limit the computational expense of path finding. In undirected settings, this maximum distance is often on the order of 3-5 [Chamberlain et al., 2023]. In directed settings, this maximum may need to be larger to account for the fact that $d_{dir}(u, v) \geq d_{undir}(u, v)$.

To understand the impact of a directed distance encoding on the predictive performance of GNN, we conducted an experiment where all modeling parameters were held fixed, and only the labeling trick was varied. The results are reported in Table 3. For the labeling trick, we constructed three variants of both the directed and undirected distance encodings. These variants are de3, de5, delog; which correspond to distance encodings with a maximum distance of 3, 15, and no maximum but log-transformed. The -d and -u labels indicate that the method is directed or undirected, respectively. In these experiments, we observe that the directionality provides improvements across all datasets, but the size of impact varies significantly. In the example of CORA, we observe a 50% improvement, while both CHAMELEON and BLOG have much more modest gains. Interestingly, we find that the maximum distance cutoff does not correlate in a predictable fashion with performance. Based on these results, we conclude that directionality should be accounted for when using a labeling trick during modeling, and that the maximum distance cutoff should be carefully tuned.

Table 3: Comparison of undirected and directed labeling tricks in terms of MRR.

<i>Labeling</i>	CORA	CHAMELEON	BLOG
de3-u	0.283±0.044	0.398±0.069	0.137±0.024
de15-u	0.324±0.049	0.385±0.109	0.116±0.031
delog-u	0.270±0.049	0.392±0.116	0.120±0.017
de3-d	0.498±0.071	0.289±0.102	0.160±0.023
de15-d	0.493±0.067	0.405±0.065	0.125±0.035
delog-d	0.305±0.050	0.397±0.077	0.109±0.027

Directed vs Undirected Negative Sampling. We next turn our attention to exploring the effects of directionality in negative sampling. Link prediction is traditionally constructed as a binary classification task, where positive samples are observed edges and negative samples are unobserved edges. Enumerating all negative samples is intractable, so it is common to sample a subset of those negatives for training. It is possible to generate negative samples in either a directed or an undirected fashion. Directed negative sampling generates a dataset $\mathcal{D}^n = \{(u, v) : u, v \sim \mathcal{V}\}$ with $(u, v) \neq (v, u)$. In undirected negative sampling, $\mathcal{D}^n = \{(u, v) : u, v \sim \mathcal{V}\}$ with $(u, v) = (v, u)$.

To explore this design principle, we constructed an experiment where we held the model parameters fixed, and altered only the negative sampling strategy. In this experiment we used DirGNN as the encoder, CMLP as the decoder, de15 as the labeling method, and all structural features. The results for this experiment are presented in Table 4. We note across all three datasets that directed negative sampling provides a lift in MRR, although in two of the three datasets, the lift is modest. We conclude that there is evidence to support the usage of directed negative sampling, but that these effects are smaller than other design principles.

Table 4: Comparison of undirected and directed negative sampling in terms of MRR.

<i>Sampling</i>	CORA	CHAMELEON	BLOG
Undirected	0.48±0.12	0.60±0.07	0.27±0.03
Directed	0.50±0.09	0.61±0.03	0.28±0.02

Directed vs Undirected Structural Features. Previous work has shown that the inclusion of edge-wise structural features, such as the number of shared common neighbors at k-hops, leads to significant performance improvements for link prediction [Zhang et al., 2024, Ai et al., 2022, Zhang and Chen, 2018]. Indeed, this intuitively makes sense because these structural features are the building blocks for heuristic similarity measures such as Adamic-Adar or Resource-Allocation, both of which represent strong baselines in undirected link prediction settings. The definition of our structural features can be found in Equations 14-17.

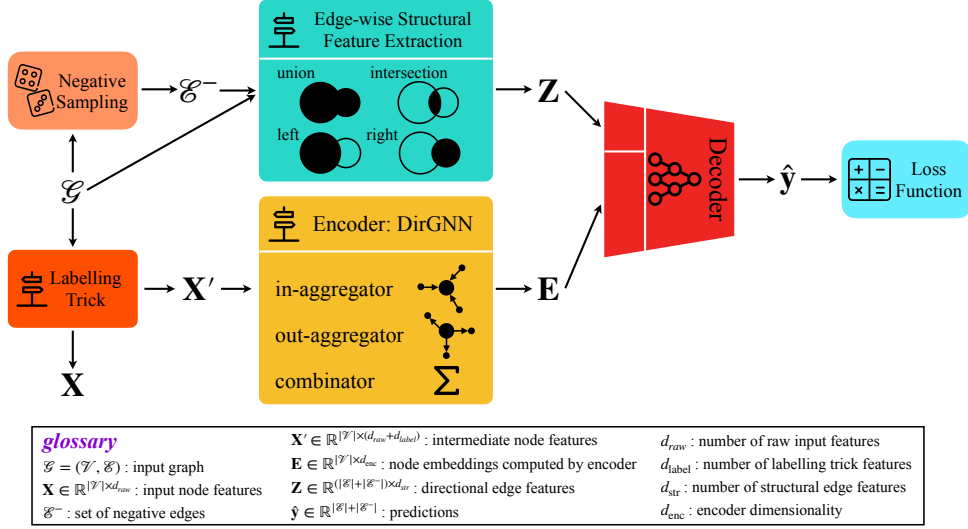


Figure 2: **Overview of DirLP.** Given the input graph $\mathcal{G} = (\mathcal{V}, \mathcal{E})$ and node features $\mathbf{x} \in \mathbb{R}^{d_{\text{raw}}}, \forall u \in \mathcal{V}$, DirLP follows a series of steps to predict directed links. First, a set of negative edges \mathcal{E}^- is generated. Next, for each edge (u, v) in the set $\mathcal{E} \cup \mathcal{E}^-$, structural edge features $\mathbf{z}_{(u,v)} \in \mathbb{R}^{d_{\text{str}}}$ are computed. Then, directional labels are assigned to each node $u \in \mathcal{V}$, and intermediate node features $\mathbf{x}'_u \in \mathbb{R}^{d_{\text{raw}} + d_{\text{label}}}$ are constructed by concatenating the original node features with the directional labels. The model then applies DirGNN message passing to produce node embeddings $\mathbf{e}_u \in \mathbb{R}^{d_{\text{enc}}}$ for $u \in \mathcal{V}$. For each edge (u, v) in $\mathcal{E} \cup \mathcal{E}^-$, the edge features are concatenated with the node embeddings of the edge’s endpoints. Finally, these concatenated embeddings are passed through an MLP followed by a sigmoid activation function to make predictions.

To understand whether directionality affects the performance of models that include structure features, we constructed an experiment where we used DirGNN as the encoder, and CMLP as the decoder, while varying the structural features. The results are reported in Table 5. We observe that across all three datasets, directed structural features provide a significant improvement over their undirected variants. In percentage-increase terms, we find an uplift of 30% to 50% through the inclusion of directionality, indicating that this is a significant design principle. The improvement is larger than the associated uncertainties, giving us confidence that this improvement is robust.

Table 5: Comparison of undirected and directed structural features in terms of MRR.

<i>SFs</i>	CORA	CHAMELEON	BLOG
undirected	0.309±0.051	0.348±0.020	0.174±0.020
directed	0.412±0.064	0.534±0.038	0.251±0.033

5 Proposed Model

Based on the insights drawn through the experiments conducted on analyzing directionality, we propose a framework, namely *DirLP*, for directed link prediction. DirLP features the following key components: A directed labeling trick, a directed encoder, a directed structure feature extractor, and an asymmetric decoder. An overview of model architecture is provided in Figure 2. In the remainder of this section, we describe each element and how they’re combined to form DirLP.

We begin with the **directed labeling trick**, which injects structural information into our graph encoder, and is defined as:

$$\mathbf{1}_t = \left[d^\delta(t, v) \parallel d^\delta(t, v) \forall v \in \mathcal{V} \right], \quad (9)$$

where d^δ is the truncated graph distance defined as $d^\delta(t, v) = \min(\delta, d(t, v))$, t is the landmark vertex, and δ is the maximum distance. For DirLP, we use two fixed landmarks.

Table 6: Comparison of baseline methods and our proposed model in terms MRR on directed link prediction task. The top three models are highlighted as **First**, **Second**, **Third**. Note that The Blog dataset does not have vertex features and therefore MLP model built from vertex features do not apply.

	CORA	CITESEER	CHAMELEON	SQUIRREL	BLOG	WIKICS
LP, sym	0.315±0.065	0.303±0.073	0.235±0.013	0.102±0.005	0.096±0.021	0.661±0.011
LP, asym	0.324±0.056	0.146±0.024	0.381±0.075	0.497±0.151	0.149±0.030	0.424±0.067
RA, sym	0.356±0.07	0.293±0.049	0.194±0.069	0.087±0.013	0.082±0.021	0.358±0.074
RA, asym	0.292±0.046	0.134±0.021	0.353±0.142	0.148±0.037	0.103±0.024	0.494±0.101
AA, sym	0.353±0.067	0.254±0.048	0.239±0.016	0.103±0.005	0.096±0.023	0.285±0.033
AA, asym	0.288±0.045	0.122±0.02	0.378±0.091	0.495±0.196	0.143±0.034	0.487±0.060
MLP	0.172±0.03	0.356±0.084	0.104±0.029	0.051±0.027	-	0.019±0.006
GAT	0.087±0.036	0.115±0.043	0.150±0.026	0.088±0.038	0.057±0.011	0.094±0.010
GCN	0.402±0.062	0.208±0.048	0.270±0.043	0.260±0.018	0.080±0.025	0.277±0.047
GraphSage	0.414±0.077	0.158±0.063	0.202±0.046	0.190±0.074	0.083±0.016	0.185±0.058
DirLP	0.504±0.088	0.480±0.108	0.657±0.037	0.759±0.012	0.280±0.031	0.752±0.028

We utilize **Directed Graph Neural Network (DirGNN) as encoder**, which aggregates messages from incoming and outgoing edges separately for each node, and obtain layer updates by a non-parametric combinator function [Rossi et al., 2024]. More formally, DirGNN initializes the hidden node embeddings by intermediate node features, i.e., $\mathbf{h}_u^{(0)} = \mathbf{x}'_u$ for all $u \in \mathcal{V}$. With our choices of aggregation and update functions, GraphSage [Hamilton et al., 2017] and convex combination [Rossi et al., 2024], respectively, at the k^{th} layer of encoder node embeddings $\mathbf{h}_u^{(k)}$ are updated as follows:

$$\mathbf{m}_{u,\text{in}}^{(k+1)} = \mathbf{W}_{\text{in,self}}^{(k)} \mathbf{h}_u^{(k)} + \mathbf{W}_{\text{in}}^{(k)} \frac{\sum_{v \in \mathcal{N}_{\text{in}}(u)} \mathbf{h}_v^{(k)}}{|\mathcal{N}_{\text{in}}(u)|}, \quad (10)$$

$$\mathbf{m}_{u,\text{out}}^{(k+1)} = \mathbf{W}_{\text{out,self}}^{(k)} \mathbf{h}_u^{(k)} + \mathbf{W}_{\text{out}}^{(k)} \frac{\sum_{v \in \mathcal{N}_{\text{out}}(u)} \mathbf{h}_v^{(k)}}{|\mathcal{N}_{\text{out}}(u)|}, \quad (11)$$

$$\mathbf{h}_u^{(k+1)} = \alpha \times \mathbf{m}_{u,\text{in}}^{(k+1)} + (1 - \alpha) \times \mathbf{m}_{u,\text{out}}^{(k+1)}, \quad (12)$$

where $\mathbf{W}_{\text{in}}^{(k)}$, $\mathbf{W}_{\text{in,self}}^{(k)}$, $\mathbf{W}_{\text{out}}^{(k)}$, $\mathbf{W}_{\text{out,self}}^{(k)}$ are learnable parameters and α is a hyperparameter that controls the trade-off of emphasis between incoming and outgoing edges. In our experiments, we set $\alpha = 0.5$ for all datasets to equally treat directions. The node embeddings are set to final layer output, i.e., $\mathbf{e}_u = \mathbf{h}_u^{(K)}$, $\forall u \in \mathcal{V}$, where K denotes the total number of update layers.

We perform **edge-wise structural feature extraction** to incorporate the directionally aware structural information at the edge-level. We define a set of *neighbourhood directionality sequences* at length n , $\mathbb{S}_n = \{(s_1, \dots, s_n) : \forall s_i \in \{\text{in}, \text{out}\}\}$. Now, for a given node u and directionality sequence $\mathbf{s} = (s_1, \dots, s_n)$, we define directional neighbourhood $\mathcal{N}_{\mathbf{s}}^{\text{dir}}(u)$ such that $v \in \mathcal{N}_{\mathbf{s}}^{\text{dir}}(u)$, if and only if v is reachable from u with an n -step walk where i^{th} step is in the direction of s_i . For an edge (u, v) , we compute the cardinality of the union (U) and intersection (I) of the directed neighborhoods of endpoints, in addition to the individual neighbourhoods of left (L) and right (R) side as follows:

$$\mathbf{z}_{(u,v)}^{\text{U}} = [|\mathcal{N}_{\mathbf{s}_1}(u) \cup \mathcal{N}_{\mathbf{s}_2}(v)|]_{\mathbf{s}_1, \mathbf{s}_2 \in \bigcup_{n=1}^N \mathbb{S}_n}, \quad (13)$$

$$\mathbf{z}_{(u,v)}^{\text{L}} = [|\mathcal{N}_{\mathbf{s}}(u)|]_{\mathbf{s} \in \bigcup_{n=1}^N \mathbb{S}_n}, \quad (14)$$

$$\mathbf{z}_{(u,v)}^{\text{I}} = [|\mathcal{N}_{\mathbf{s}_1}(u) \cap \mathcal{N}_{\mathbf{s}_2}(v)|]_{\mathbf{s}_1, \mathbf{s}_2 \in \bigcup_{n=1}^N \mathbb{S}_n}, \quad (15)$$

$$\mathbf{z}_{(u,v)}^{\text{R}} = [|\mathcal{N}_{\mathbf{s}}(v)|]_{\mathbf{s} \in \bigcup_{n=1}^N \mathbb{S}_n}, \quad (16)$$

$$\mathbf{z}_{(u,v)}^{\text{dir}} = \mathbf{z}_{(u,v)}^{\text{U}} \parallel \mathbf{z}_{(u,v)}^{\text{I}} \parallel \mathbf{z}_{(u,v)}^{\text{L}} \parallel \mathbf{z}_{(u,v)}^{\text{R}}, \quad (17)$$

where N is the maximum radius. Next, we compute the undirected versions over symmetrized adjacency matrix that define neighbourhood $\mathcal{N}_k(u)$ which involves nodes at k -hop distance to a given node u :

$$\mathbf{z}_{(u,v)}^{\text{undir}} = [|\mathcal{N}_k(u) \cup \mathcal{N}_k(v)|]_{k=1}^N \parallel [|\mathcal{N}_k(u) \cap \mathcal{N}_k(v)|]_{k=1}^N \parallel [|\mathcal{N}_k(u)|]_{k=1}^N \parallel [|\mathcal{N}_k(v)|]_{k=1}^N. \quad (18)$$

Finally, the complete edge feature vector is obtained by concatenating the directed and undirected structural features; $\mathbf{z}_{(u,v)} = \mathbf{z}_{(u,v)}^{\text{dir}} \parallel \mathbf{z}_{(u,v)}^{\text{undir}}$.

We employ a simple **feedforward network as decoder** that concatenates the edge features and node embeddings of source and target node and performs linear transformations through a *Multi-layer Perceptron (MLP)*:

$$\hat{y}_{u,v} = \sigma \left(f_{\text{MLP}} \left(\mathbf{z}_{u,v} \parallel \mathbf{e}_u \parallel \mathbf{e}_v \right) \right), \quad (19)$$

where $f_{\text{MLP}}(\cdot)$ is a feed forward network and σ is the sigmoid function.

Expressivity. Being able to represent edge direction through an asymmetric decoder and including information about directed triangle counts, DirLP is capable of distinguishing edges that conventional MPNNs are not able to which is stated by Theorem 1.

Theorem 1. *Let $\mathcal{M}_{\text{sGNN}}$ be the family of GNNs defined by Equation 7 equipped with a symmetric decoder and augmented by undirected structural features. Additionally, let $\mathcal{M}_{\text{DirLP}}$ be family of all models defined by Equation 19. $\mathcal{M}_{\text{DirLP}}$ is strictly more powerful than $\mathcal{M}_{\text{sGNN}}$ ($\mathcal{M}_{\text{sGNN}} \subset \mathcal{M}_{\text{DirLP}}$).*

This makes intuitive sense because our asymmetric decoder can represent all symmetric decoders, which allows DirLP to distinguish all links any symmetric GNNs can. We present the proof in Appendix C.

6 Principle Comparison

Setup. In our experiments, we generated ten sets of random splits of datasets for training, validation, and testing to facilitate 10-fold cross-validation. These dataset splits will be made publicly available upon official publication of this work. Each of the deep-learning models was optimized using the hyperparameter tuning framework OPTUNA [Akiba et al., 2019], with 48 optimization steps performed per model to find the best-performing configurations. The optimization process was conducted on the validation set focusing on the Mean Reciprocal Rank (MRR). The search space of OPTUNA and tuned hyperparameter settings for all deep-learning models are provided in Appendix E. Experiments were run on an NVIDIA DGX A100 machine with 128 AMD ROME 7742 cores and 8 NVIDIA A100 GPUs, utilizing PYTORCH GEOMETRIC 2.5.3 and PYTORCH 2.3.1 for model training and evaluation.

Baselines. We performed a set of principle comparison experiments between our proposed method, DirLP, and several baseline approaches, including both symmetric and asymmetric versions of similarity-based heuristics LP [Lü et al., 2009], RA [Zhou et al., 2009], and AA [Adamic and Adar, 2003], as well as four deep-learning based baselines: MLP, GAT [Veličković et al., 2017], GCN [Kipf and Welling, 2016] and GraphSage [Hamilton et al., 2017]. The implementations of deep-learning models were based on official code provided in PYTORCH GEOMETRIC 2.5.3, ensuring consistency and reproducibility.

Results. The main results of our principle comparison experiments are presented in Table 6 in terms of MRR. Additionally, in Appendix D, we report the performance comparison in terms of Hits@20 in the Appendix in Table 8. Based on these results, we draw several important conclusions. First, we observe that the asymmetric versions of heuristic methods consistently outperform their symmetric counterparts on datasets such as CHAMELEON, SQUIRREL, BLOG, and WIKICS, with the only exception of LP on WIKICS. Reviewing the dataset statistics reported in Appendix A, we find a positive correlation between graph density and the performance advantage of using asymmetric methods. This suggests that as the complexity of the graph structure increases, the inclusion of directional information becomes more critical.

In all cases, heuristic methods outperform deep-learning baselines that do not incorporate directionality in the message-passing framework. This finding suggests that incorporating edge directionality can have a greater impact than increasing model complexity, particularly in many settings. Deep-learning baselines perform poorly, especially in cases where the node features offer limited information. For instance, on datasets BLOG and WIKICS, which have relatively low vertex feature dimensionality compared to other datasets (see Appendix A), heuristic methods significantly outperform the deep-learning baselines. This highlights the importance of effectively modeling directionality in graph structure when node features are insufficient.

The principle comparison experiments clearly demonstrate the superiority of DirLP, which captures directionality through message-passing mechanisms and feature extraction both at the edge and node level. In many instances, DirLP delivers significantly superior performance compared to deep-learning baselines, highlighting its ability to model directional relationships more effectively.

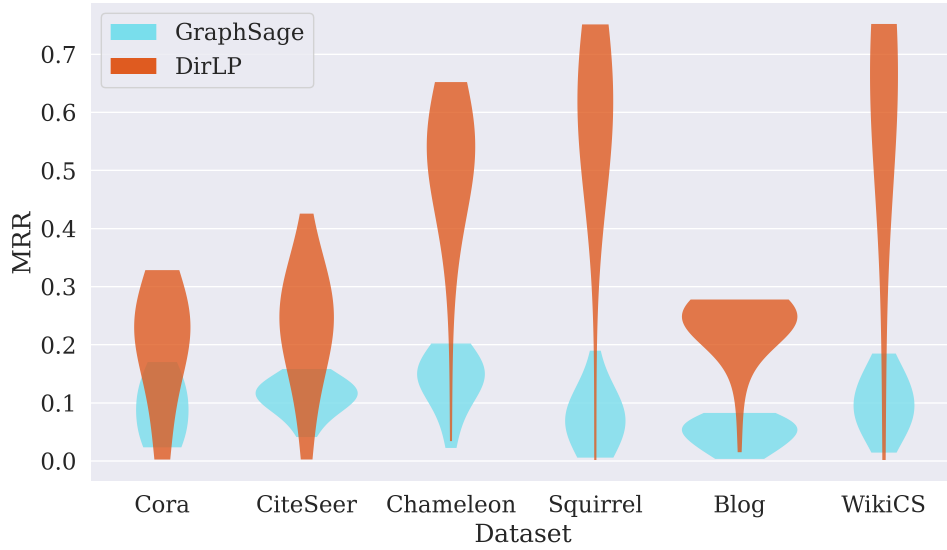


Figure 3: **Statistical Comparison Between GraphSage and DirLP.** The violin plots illustrate the performance of GraphSage and DirLP in terms of MRR across multiple data splits.

Sensitivity. A violin plot ³ illustrating the comparison between DirLP and GraphSage, in terms of MRR, is shown in Figure 3, offering further insights into the model’s performance distribution across the data splits. It is observed that DirLP shows higher variance, however on the average it outperforms GraphSage clearly.

7 Conclusion

In conclusion, this paper introduces DirLP, a novel framework for directed link prediction that outperforms existing models across benchmark datasets. By leveraging an asymmetric decoder and directed structural features, DirLP effectively captures relationships in graphs where edge directionality is critical, highlighting the limitations of traditional undirected methods.

Rather than introducing a complex new architecture, our work focuses on systematically exploring the utility of simple, directed variants of existing techniques. Directed distance encoding and directed GNNs, though seemingly minor modifications, demonstrate substantial performance gains, emphasizing the practical value of incorporating directionality. This study serves as a guide for practitioners, showing how fundamental, interpretable methods can deliver strong results in directed settings.

While scalability remains a consideration due to preprocessing costs of edge-wise structural feature extraction, these are one-time operations that can be optimized. Future work will focus on enhancing the efficiency of our approach and extending evaluations to larger datasets to broaden its applicability.

This work sets a benchmark for directed link prediction and lays a foundation for future research, encouraging deeper exploration into the role of directionality and the development of scalable, high-performing solutions for directed graph tasks.

Acknowledgments

All funding was provided by Block Inc. ⁴.

³Violin plots provides a visual summary of the data distribution along with its probability density that is smoothed and symmetrized by a Kernel density estimation (KDE).

⁴block.xyz

References

- Evrin Acar, Daniel M Dunlavy, and Tamara G Kolda. Link prediction on evolving data using matrix and tensor factorizations. In *Proc. IEEE Int. Conf. Data Mining (ICDM) Workshops*, pages 262–269, 2009.
- Lada A Adamic and Eytan Adar. Friends and neighbors on the web. *Social Networks*, 25, 2003.
- Baole Ai, Zhou Qin, Wenting Shen, and Yong Li. Structure enhanced graph neural networks for link prediction. *arXiv preprint arXiv:2201.05293*, 2022.
- Takuya Akiba, Shotaro Sano, Toshihiko Yanase, Takeru Ohta, and Masanori Koyama. Optuna: A next-generation hyperparameter optimization framework. In *Proc. ACM SIGKDD Int. Conf. Knowledge Discovery and Data Mining*, pages 2623–2631, 2019.
- Zhu Cao, Linlin Wang, and Gerard De Melo. Link prediction via subgraph embedding-based convex matrix completion. In *Proc. AAAI Conf. Artificial Intelligence*, 2018.
- Benjamin Paul Chamberlain, Sergey Shirobokov, Emanuele Rossi, Fabrizio Frasca, Thomas Markovich, Nils Hammerla, Michael M Bronstein, and Max Hansmire. Graph neural networks for link prediction with subgraph sketching. *arXiv preprint arXiv:2209.15486*, 2022.
- Benjamin Paul Chamberlain, Sergey Shirobokov, Emanuele Rossi, Fabrizio Frasca, Thomas Markovich, Nils Yannick Hammerla, Michael M. Bronstein, and Max Hansmire. Graph neural networks for link prediction with subgraph sketching. In *The Eleventh International Conference on Learning Representations*, 2023. URL <https://openreview.net/forum?id=m1oqE0AozQU>.
- Aaron Clauset, Cristopher Moore, and Mark EJ Newman. Hierarchical structure and the prediction of missing links in networks. *Nature*, 453(7191):98–101, 2008.
- Ahmed El-Kishky, Thomas Markovich, Serim Park, Chetan Verma, Baekjin Kim, Ramy Eskander, Yury Malkov, Frank Portman, Sofia Samaniego, Ying Xiao, et al. Twhin: Embedding the twitter heterogeneous information network for personalized recommendation. In *Proc. ACM SIGKDD Int. Conf. Knowledge Discovery and Data Mining*, pages 2842–2850, 2022.
- Simon Geisler, Yujia Li, Daniel J Mankowitz, Ali Taylan Cemgil, Stephan Günnemann, and Cosmin Paduraru. Transformers meet directed graphs. In *Proc. Int. Conf. Machine Learning (ICML)*, pages 11144–11172, 2023.
- Roger Guimerà and Marta Sales-Pardo. Missing and spurious interactions and the reconstruction of complex networks. *Proceedings of the National Academy of Sciences*, 106(52):22073–22078, 2009.
- Will Hamilton, Zitao Ying, and Jure Leskovec. Inductive representation learning on large graphs. *Advances in Neural Information Processing Systems*, 30, 2017.
- Yixuan He, Gesine Reinert, and Mihai Cucuringu. Digrac: Digraph clustering based on flow imbalance. In *Proc. Learning on Graphs Conference*, pages 21:1–21:43, 2022.
- Yixuan He, Xitong Zhang, Junjie Huang, Benedek Rozemberczki, Mihai Cucuringu, and Gesine Reinert. Pytorch geometric signed directed: A software package on graph neural networks for signed and directed graphs. In *Proc. Learning on Graphs Conference*, pages 12–1, 2024.
- Seyed Mehran Kazemi and David Poole. Simple embedding for link prediction in knowledge graphs. *Advances in Neural Information Processing Systems*, 31, 2018.
- Thomas N Kipf and Max Welling. Semi-supervised classification with graph convolutional networks. *arXiv preprint arXiv:1609.02907*, 2016.
- Pan Li, Yanbang Wang, Hongwei Wang, and Jure Leskovec. Distance encoding: Design provably more powerful neural networks for graph representation learning. *Advances in Neural Information Processing Systems*, 33:4465–4478, 2020.
- Yujia Li, Daniel Tarlow, Marc Brockschmidt, and Richard Zemel. Gated graph sequence neural networks. *arXiv preprint arXiv:1511.05493*, 2015.
- David Liben-Nowell and Jon Kleinberg. The link-prediction problem for social networks. *J. American Society for Information Science and Technology*, 2007.
- Zhiwei Liu, Yingdong Dou, Philip S Yu, Yutong Deng, and Hao Peng. Alleviating the inconsistency problem of applying graph neural network to fraud detection. In *Proc. Int. ACM SIGIR Conf. Research and Development in Information Retrieval*, pages 1569–1572, 2020.
- Linyuan Lü, Ci-Hang Jin, and Tao Zhou. Similarity index based on local paths for link prediction of complex networks. *Phys. Rev. E*, 80:046122, 2009.

- Yi Ma, Jianye Hao, Yaodong Yang, Han Li, Junqi Jin, and Guangyong Chen. Spectral-based graph convolutional network for directed graphs. *arXiv preprint arXiv:1907.08990*, 2019.
- Péter Mernyei and Cătălina Cangea. Wiki-cs: A wikipedia-based benchmark for graph neural networks. In *Proc. ICML Graph Representation Learning and Beyond workshop*, 2020.
- Federico Monti, Karl Otness, and Michael M Bronstein. Motifnet: a motif-based graph convolutional network for directed graphs. In *Proc. IEEE Data Science Workshop*, pages 225–228, 2018.
- M. E. J. Newman. Clustering and preferential attachment in growing networks. *Physical Review E*, 2001.
- Mingdong Ou, Peng Cui, Jian Pei, Ziwei Zhang, and Wenwu Zhu. Asymmetric transitivity preserving graph embedding. In *Proc. ACM SIGKDD Int. Conf. Knowledge Discovery and Data Mining*, pages 1105–1114, 2016.
- Aditya Pal, Chantat Eksombatchai, Yitong Zhou, Bo Zhao, Charles Rosenberg, and Jure Leskovec. Pinnnersage: Multi-modal user embedding framework for recommendations at pinterest. In *Proceedings of the 26th ACM SIGKDD International Conference on Knowledge Discovery & Data Mining*, pages 2311–2320, 2020.
- Bryan Perozzi, Rami Al-Rfou, and Steven Skiena. Deepwalk: Online learning of social representations. In *Proc. ACM SIGKDD Int. Conf. Knowledge Discovery and Data Mining*, pages 701–710, 2014.
- Emanuele Rossi, Bertrand Charpentier, Francesco Di Giovanni, Fabrizio Frasca, Stephan Günnemann, and Michael M Bronstein. Edge directionality improves learning on heterophilic graphs. In *Proc. Learning on Graphs Conference*, pages 25–1, 2024.
- Benedek Rozemberczki, Carl Allen, and Rik Sarkar. Multi-scale attributed node embedding. *J. Complex Networks*, 9(2), 2021.
- Guillaume Salha, Stratis Limnios, Romain Hennequin, Viet-Anh Tran, and Michalis Vazirgiannis. Gravity-inspired graph autoencoders for directed link prediction. In *Proc. ACM Int. Conf. Information and Knowledge Management*, pages 589–598, 2019.
- Richard Socher, Danqi Chen, Christopher D Manning, and Andrew Ng. Reasoning with neural tensor networks for knowledge base completion. *Advances in Neural Information Processing Systems*, 26, 2013.
- Balasubramaniam Srinivasan and Bruno Ribeiro. On the equivalence between positional node embeddings and structural graph representations. *arXiv preprint arXiv:1910.00452*, 2019.
- Jian Tang, Meng Qu, Mingzhe Wang, Ming Zhang, Jun Yan, and Qiaozhu Mei. Line: Large-scale information network embedding. In *Proc. Int. Conf. World Wide Web (WWW)*, pages 1067–1077, 2015.
- Zekun Tong, Yuxuan Liang, Changsheng Sun, Xinke Li, David Rosenblum, and Andrew Lim. Digraph inception convolutional networks. *Advances in neural information processing systems*, 33:17907–17918, 2020a.
- Zekun Tong, Yuxuan Liang, Changsheng Sun, David S Rosenblum, and Andrew Lim. Directed graph convolutional network. *arXiv preprint arXiv:2004.13970*, 2020b.
- Théo Trouillon, Johannes Welbl, Sebastian Riedel, Éric Gaussier, and Guillaume Bouchard. Complex embeddings for simple link prediction. In *Proc. Int. Conf. Machine Learning (ICML)*, pages 2071–2080, 2016.
- Petar Veličković, Guillem Cucurull, Arantxa Casanova, Adriana Romero, Pietro Lio, and Yoshua Bengio. Graph attention networks. *arXiv preprint arXiv:1710.10903*, 2017.
- Lovro Vršek, Xavier Bresson, Thomas Laurent, Martin Schmitz, and Mile Šikić. Learning to untangle genome assembly with graph convolutional networks. *arXiv preprint arXiv:2206.00668*, 2022.
- Chao Wang, Venu Satuluri, and Srinivasan Parthasarathy. Local probabilistic models for link prediction. In *Proc. IEEE Int. Conf. Data Mining (ICDM)*, pages 322–331, 2007.
- Yuening Wang, Yingxue Zhang, Antonios Valkanias, Ruiming Tang, Chen Ma, Jianye Hao, and Mark Coates. Structure aware incremental learning with personalized imitation weights for recommender systems. In *Proc. AAAI Conf. Artificial Intelligence*, 2023.
- Bishan Yang, Wen-tau Yih, Xiaodong He, Jianfeng Gao, and Li Deng. Embedding entities and relations for learning and inference in knowledge bases. *arXiv preprint arXiv:1412.6575*, 2014.
- Zhilin Yang, William W. Cohen, and Ruslan Salakhutdinov. Revisiting semi-supervised learning with graph embeddings. In *Proc. Int. Conf. Machine Learning (ICML)*, 2016.
- Rex Ying, Ruining He, Kaifeng Chen, Pong Eksombatchai, William L Hamilton, and Jure Leskovec. Graph convolutional neural networks for web-scale recommender systems. In *Proc. ACM SIGKDD Int. Conf. Knowledge Discovery and Data Mining*, pages 974–983, 2018.

- Ge Zhang, Zhao Li, Jiaming Huang, Jia Wu, Chuan Zhou, Jian Yang, and Jianliang Gao. efraudcom: An e-commerce fraud detection system via competitive graph neural networks. *ACM Trans. Information Systems (TOIS)*, 40(3):1–29, 2022.
- Muhan Zhang and Yixin Chen. Link prediction based on graph neural networks. *Advances in neural information processing systems*, 31, 2018.
- Muhan Zhang, Pan Li, Yinglong Xia, Kai Wang, and Long Jin. Labeling trick: A theory of using graph neural networks for multi-node representation learning. *Advances in Neural Information Processing Systems*, 34:9061–9073, 2021a.
- Tianyi Zhang, Haoteng Yin, Rongzhe Wei, Pan Li, and Anshumali Shrivastava. Learning scalable structural representations for link prediction with bloom signatures. In *Proceedings of the ACM on Web Conference 2024*, pages 980–991, 2024.
- Xitong Zhang, Yixuan He, Nathan Brugnone, Michael Perlmutter, and Matthew Hirn. Magnet: A neural network for directed graphs. *Advances in neural information processing systems*, 34:27003–27015, 2021b.
- Tao Zhou, Linyuan Lü, and Yi-Cheng Zhang. Predicting missing links via local information. *The European Physical Journal B*, 71:623–630, 2009.

A Dataset Details

In our experiments, we evaluate directed link prediction performance of various approaches using six benchmark datasets: CORA [Yang et al., 2016], CITESEER [Yang et al., 2016], CHAMELEON [Rozemberczki et al., 2021], SQUIRREL [Rozemberczki et al., 2021], BLOG [He et al., 2022], WIKICS [Mernyei and Cangea, 2020]. CORA and CITESEER are citation networks where the nodes denote the papers and links denote the citations from one to another. Likewise, CHAMELEON, SQUIRREL and WIKICS are reference networks on Wikipedia pages in the corresponding topics where edges reflect reference links between them. BLOG is a set of political blogs from the 2004 US presidential election with links recording mentions between them.

Table 7: Dataset Statistics. d , $|\mathcal{V}|$, $|\mathcal{E}|$, $|\mathcal{E}_{\leftrightarrow}|/|\mathcal{E}|$, denote the number of node features, number of nodes, number of edges and ratio of node pairs connected in both direction to total number of edges, respectively. Graph density is calculated by $|\mathcal{E}|/(|\mathcal{V}| \times (|\mathcal{V}| - 1))$.

	CORA	CITESEER	CHAMELEON	SQUIRREL	BLOG	WIKICS
d	1,433	3,703	2,325	2,089	0	300
$ \mathcal{V} $	2,708	3,327	2,277	5,201	1,222	11,701
$ \mathcal{E} $	10,556	9,104	36,101	217,073	19,024	297,110
$ \mathcal{E}_{\leftrightarrow} / \mathcal{E} $	6.1%	4.9%	26%	17%	24%	52%
Density	0.1%	0.1%	0.7%	0.8%	1.3%	0.2%

B Heuristics Formulations

In our experiments we use three different node similarity scores and their directed variants; local path index (LP), resource allocation index (RA), Adamic-Adar index (AA). Their original formulations (symmetric versions) are formulated as follows for a pair of nodes $u, v \in \mathcal{V}$:

$$S_{\text{LP,sym}}(u, v) = \hat{\mathbf{A}}_{u,v}^2 + \epsilon \hat{\mathbf{A}}_{u,v}^3, \quad (20)$$

$$S_{\text{RA,sym}}(u, v) = \sum_{t \in \mathcal{N}(u) \cap \mathcal{N}(v)} \frac{1}{|\mathcal{N}(t)|}, \quad (21)$$

$$S_{\text{AA,sym}}(u, v) = \sum_{t \in \mathcal{N}(u) \cap \mathcal{N}(v)} \frac{1}{\log |\mathcal{N}(t)|}, \quad (22)$$

where $\hat{\mathbf{A}}$ denotes the symmetrized adjacency matrix and ϵ is a free parameter set to 10^{-3} in our experiments. Asymmetric variant of LP is simply defined as follows:

$$S_{\text{LP,asym}}(u, v) = \mathbf{A}_{u,v}^2 + \epsilon \mathbf{A}_{u,v}^3. \quad (23)$$

Recall the definition for directed neighborhood operator:

$$\mathcal{N}_{\text{in}}(u) = \{v \in \mathcal{V} \mid (v, u) \in \mathcal{E}\}, \quad \mathcal{N}_{\text{out}}(u) = \{v \in \mathcal{V} \mid (u, v) \in \mathcal{E}\}, \quad (24)$$

where $\mathcal{N}_{\text{in}}(u)$ ($\mathcal{N}_{\text{out}}(u)$) consists of all nodes that have a directed edge pointing toward (originating from) node u . The four directional variants of AA and RA for a given node pair u and v follows:

$$S_{\text{RA}, d_u-d_v}(u, v) = \sum_{t \in \mathcal{N}_{d_u}(u) \cap \mathcal{N}_{d_v}(v)} \frac{1}{|\mathcal{N}(t)|}, \quad (25)$$

$$S_{\text{AA}, d_u-d_v}(u, v) = \sum_{t \in \mathcal{N}_{d_u}(u) \cap \mathcal{N}_{d_v}(v)} \frac{1}{\log |\mathcal{N}(t)|}. \quad (26)$$

The asymmetric variants of AA and RA on our baseline experiments are selected based on best performing version of directed common neighbourhood operator.

C Proof of Theorem 1

Our proof follows two steps. First, we show that $\mathcal{M}_{\text{sGNN}} \subseteq \mathcal{M}_{\text{DirLP}}$. Next, Then, we construct a graph that exhibits an automorphic nodal structure for all elements of $\mathcal{M}_{\text{sGNN}}$, but not for any element of $\mathcal{M}_{\text{DirLP}}$.

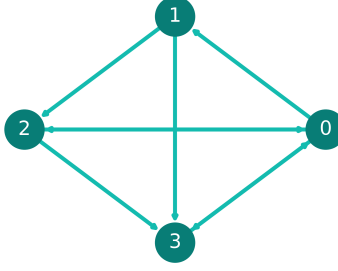


Figure 4: A complete graph with four nodes.

The first half of the proof can be seen by examining the structure of DirLP, and the way in which it generalizes a GNN with a symmetric decoder and symmetric structural features. The general form for a sGNN is given by:

$$f_{\text{sGNN}} = f_{\text{mlp}}(\mathbf{z}_{u,v}^{\text{undir}} || \mathbf{e}_u \odot \mathbf{e}_v). \quad (27)$$

Starting from Equation 19, we see immediately that we can recover a symmetric for decoder for $\mathbf{e}_u || \mathbf{e}_v$ by selecting an initial layer that corresponds to two concatenated identity matrices. Turning our attention to the structural features, we again see that a special combination of the elements of $\mathbf{z}_{u,v}$ allows us to recover $\mathbf{z}_{u,v}^{\text{undir}}$. Namely, a trace over all modes allows us to construct the undirected structural features. This amounts to using a matrix of all 1s for the initial layer of our MLP. Putting this all together, we observe that we can convert our set of directed input features to their undirected variants using an MLP whose initial weight matrix is equal to $[\mathbf{B} || \mathbf{I}_{D \times D} || \mathbf{I}_{D \times D}]$, where \mathbf{B} is the desired trace matrix. Therefore, because there exists a DirLP that is equivalent to a sGNN, any edge that is distinguished by an sGNN must also be distinguishable by a DirLP. This is sufficient to prove that $\mathcal{M}_{\text{sGNN}} \subseteq \mathcal{M}_{\text{DirLP}}$.

We next turn to the task of making this relationship strict, which we do by constructing a graph for which sGNN cannot distinguish a node pair but DirLP can. To do this, we consider a complete graph with four nodes as shown in Figure 4 and consider the edges (v_0, v_1) and v_0, v_3 . In the undirected setting, all vertices exist in the same orbit, which means that no MPNN will be able to distinguish these two edges [Srinivasan and Ribeiro, 2019]. Looking further, both edges have the same structural features. As a result, $f_{\text{sGNN}}(v_0, v_1) = f_{\text{sGNN}}(v_0, v_3)$. In the directed setting, it is sufficient to show that $\mathbf{z}_{u,v}$ provides different representations for these two edges. Indeed, we observe that $\mathbf{z}_{0,1} = [\mathcal{N}_0^{\text{in}}, \mathcal{N}_0^{\text{out}}, \mathcal{N}_1^{\text{in}}, \mathcal{N}_1^{\text{out}} \dots] = [2, 1, 1, 2, \dots]$, while $\mathbf{z}_{0,3} = [2, 1, 3, 1, \dots]$, where we have neglected the intersection and union features for convenience. We conclude that these two representations are indeed different, which completes our proof.

D Principle Comparison in terms of Hits@20

Another popular performance metric used in link prediction is Hits@ k which measures the proportion of correct links (positive samples) ranked within the top k positions of a sorted list and formulated as follows:

$$\text{Hits}@k = \frac{1}{|\mathcal{E}_{\text{test}}|} \sum_{(u,v) \in \mathcal{E}_{\text{test}}} \mathbb{I}(\text{rank}(u, v) \leq k), \quad (28)$$

where \mathbb{I} is the indicator function that returns 1 if the condition inside is true and 0 otherwise.

Table 8: The Hits@20 for models with top MRRs in Table 6. The top three models are highlighted as **First**, **Second**, **Third**.

	CORA	CITESEER	CHAMELEON	SQUIRREL	BLOG	WIKICS
LP, sym	0.555 \pm 0.042	0.500\pm0.023	0.408 \pm 0.006	0.168 \pm 0.008	0.262 \pm 0.025	0.484 \pm 0.045
LP, asym	0.378 \pm 0.014	0.151 \pm 0.013	0.562 \pm 0.033	0.702 \pm 0.011	0.369\pm0.027	0.629 \pm 0.016
RA, sym	0.591 \pm 0.011	0.328 \pm 0.016	0.434 \pm 0.035	0.175 \pm 0.003	0.250 \pm 0.026	0.571 \pm 0.032
RA, asym	0.320 \pm 0.012	0.137 \pm 0.013	0.639\pm0.034	0.769\pm0.014	0.336 \pm 0.039	0.723\pm0.015
AA, sym	0.581 \pm 0.01	0.292 \pm 0.017	0.432 \pm 0.006	0.170 \pm 0.010	0.266 \pm 0.018	0.516 \pm 0.042
AA, asym	0.315 \pm 0.013	0.125 \pm 0.012	0.601\pm0.035	0.733\pm0.009	0.379\pm0.029	0.676\pm0.013
MLP	0.343 \pm 0.034	0.592\pm0.034	0.318 \pm 0.030	0.159 \pm 0.066	-	0.065 \pm 0.018
GAT	0.176 \pm 0.058	0.227 \pm 0.055	0.164 \pm 0.031	0.030 \pm 0.022	0.072 \pm 0.019	0.035 \pm 0.016
GCN	0.599\pm0.017	0.457 \pm 0.034	0.301 \pm 0.044	0.103 \pm 0.027	0.116 \pm 0.033	0.101 \pm 0.022
GraphSage	0.650\pm0.012	0.416 \pm 0.081	0.223 \pm 0.041	0.056 \pm 0.030	0.120 \pm 0.020	0.051 \pm 0.032
DirLP	0.767\pm0.057	0.991\pm0.012	0.727\pm0.032	0.706\pm0.013	0.384\pm0.035	0.635\pm0.053

E Hyperparameter Settings

The hyperparameter search space included several key parameters. The number of hidden layers was selected from the set 1, 2, 4, while the hidden layer dimension was chosen from 32, 64, 128. Similarly, the final layer dimension varied among 24, 48, 72. The number of attention heads was drawn from 2, 4, 8, 16. Additionally, the dropout probability was sampled from a uniform distribution between 0 and 0.9, and the learning rate was selected from a uniform distribution ranging between 0.0001 and 0.0600. In Table E tuned hyperparameter values are reported for each setting.

Table 9: Best hyperparameter settings for all experiments in Table 6.

Model	DATASET	CORA	CITESEER	CHAMELEON	SQUIRREL	BLOG	WIKICS
GAT	# of hidden layers	1	1	2	1	1	1
	hidden layer dim.	128	128	32	32	32	32
	final layer dim.	72	48	72	24	24	24
	# of heads	4	2	8	2	8	8
	dropout prob.	0.040	0.145	0.301	0.414	0.020	0.479
	learning rate	0.010	0.005	0.043	0.048	0.059	0.024
GCN	# of hidden layers	1	2	1	1	2	1
	hidden layer dim.	64	128	64	64	64	32
	final layer dim.	72	72	48	48	72	72
	dropout prob.	0.003	0.007	0.331	0.274	0.144	0.090
	learning rate	0.031	0.007	0.012	0.004	0.013	0.016
GraphSage	# of hidden layers	1	1	1	1	1	1
	hidden layer dim.	64	64	32	32	32	32
	final layer dim.	72	48	72	72	72	72
	dropout prob.	0.181	0.264	0.120	0.049	0.044	0.062
	learning rate	0.017	0.025	0.005	0.020	0.032	0.055
DirLP	# of hidden layers	1	2	2	1	2	2
	hidden layer dim.	64	128	128	64	128	128
	final layer dim.	72	48	72	48	72	24
	dropout prob.	0.063	0.027	0.154	0.034	0.020	0.130
	learning rate	0.045	0.037	0.037	0.029	0.090	0.014